Effects of stream discharge, alluvial depth and bar amplitude on hyporheic flow in pool-riffle channels

Daniele Tonina[1] and John M. Buffington[2]

Received 22 January 2010; revised 6 May 2011; accepted 17 May 2011; published 4 August 2011.

[1] Hyporheic flow results from the interaction between streamflow and channel morphology and is an important component of stream ecosystems because it enhances water and solute exchange between the river and its bed. Hyporheic flow in pool-riffle channels is particularly complex because of three-dimensional topography that spans a range of partially to fully submerged conditions, inducing both static and dynamic head variations. Hence, these channels exhibit transitional conditions of streambed pressure and hyporheic flow compared to previous studies of fully submerged, two-dimensional bed forms. Here, we conduct a series of three-dimensional simulations to investigate the effects of bed topography, depth of alluvium, and stream discharge on hyporheic flow in pool-riffle reaches with variable bed form submergence, and we propose three empirical formulae to predict the mean depth of hyporheic exchange and characteristic values of the residence time distribution (mean and standard deviation). Hyporheic exchange is predicted with a three-dimensional pumping model, and hyporheic flow is modeled as a Darcy flow. We find that the hyporheic residence time is well approximated by a lognormal distribution for both partially and entirely submerged pool-riffle topography, with the parameters of the distribution defined by the mean and variance of the log-transformed residence time. Depth of alluvium has a substantial effect on hyporheic flow when alluvial depth is less than a third of the bed form wavelength for the conditions examined.

Citation: Tonina, D., and J. M. Buffington (2011), Effects of stream discharge, alluvial depth and bar amplitude on hyporheic flow in pool-riffle channels, *Water Resour. Res., 47*, W08508, doi:10.1029/2010WR009140.

1. Introduction

[2] The hyporheic zone is a band of permeable saturated sediment surrounding rivers where surface and subsurface waters mix [e.g., *Vaux*, 1968, *Triska et al.*, 1993; *Boulton et al.* 1998; *Tonina and Buffington*, 2009a]. The hyporheic zone is a transitional area (ecotone) between the surface and groundwater domains and between aquatic and terrestrial habitats in the riparian zone [*Boulton et al.*, 1998; *Dahm et al.*, 2006; *Edwards* 1998; *Jones and Mulholland,* 2000; *NRC*, 2002]. Laterally, the hyporheic zone can extend several hundred meters into the floodplain [*Stanford and Ward*, 1988; *Malard et al.*, 2002; *Doering et al.*, 2007; *Jones et al.*, 2007]. Moreover, paleochannels can create preferential flow paths through alluvial valleys, rapidly conveying hyporheic flow away from the stream, and potentially increasing the lateral and longitudinal paths of the flow before it rejoins the downstream channel [*Harvey and Bencala*, 1993; *Brunke and Gonser*, 1997; *Kasahara and Wondzell*, 2003; *Poole et al.*, 2004]. Studies on the vertical extent of hyporheic flow show its dependence on surface hydraulics, streambed geometry and alluvium depth [*Vaux* 1968; *Storey et al.*, 2003; *Cardenas et al.*, 2004; *Gooseff et al.*, 2005; *Zarnetske et al.*, 2008; *Marzadri et al.*, 2010], factors that will be addressed here.

[3] Hyporheic flow can possess unique chemical and biological properties stemming from the mixing between groundwater and river water [*Smith et al.*, 2005; *Hill and Lymburner*, 1998]. Groundwater is usually low in oxygen and rich in reduced elements, and with relatively constant temperature that is not strongly influenced by daily and seasonal variations [*Winter et al.*, 1998]. In contrast, river water is well oxygenated, rich in oxidized elements, with water properties that are more variable due to rapid response to external inputs (e.g., changing weather conditions and solute concentration inputs that cause hourly to seasonal temporal variations in water quality and properties) [*Hill*, 2000].

[4] Hyporheic mixing creates a stratified biological environment [*Grimm and Fisher*, 1984], whose gradient depends on the extent and amount of exchange between surface and subsurface waters. This mixing creates a rich ecotone composed of benthic and groundwater species, which temporarily use the hyporheic zone mostly during the larval stage, and hypogean species, which permanently dwell in the pores of the hyporheic sediments [*Edwards*, 1998; *Maridet et al.*, 1992; *Naiman*, 1998].

[5] Hyporheic exchange also advects suspended and dissolved matter carried by the river into the surrounding

[1]Center for Ecohydraulics Research, College of Engineering-Boise, University of Idaho, Boise, Idaho, USA.
[2]Rocky Mountain Research Station, U.S. Forest Service, Boise, Idaho, USA.

Copyright 2011 by the American Geophysical Union.
0043-1397/11/2010WR009140

sediment [*Elliott and Brooks,* 1997a, 1997b; *Packman et al.*, 2000]. Previous laboratory studies of two-dimensional, sand-bed morphologies (ripples, dunes) show that this advective process is much stronger than molecular diffusion, and that variations in bed topography create pressure head differences on the riverbed that trigger hyporheic flow [*Vaux,* 1962, 1968; *Savant et al.*, 1987; *Thibodeaux and Boyle*, 1987; *Elliott and Brooks,* 1997a, 1997b; *Packman et al.*, 2000; *Marion et al.*, 2002; *Cardenas and Wilson*, 2007a, 2007b]. Areas of the riverbed with high pressure are characterized by downwelling fluxes in which surface water enters the sediment, and low-pressure areas exhibit upwelling fluxes in which subsurface water enters the river [*Vittal et al.*, 1977; *Savant et al.*, 1987].

[6] The above studies demonstrate that bed form topography is a key factor in controlling upwelling and downwelling fluxes, hyporheic residence time and the extent of the hyporheic zone. However, these studies have generally focused on fully submerged two-dimensional bed forms, where dynamic head variations drive the hyporheic exchange [e.g., *Vaux,* 1962, 1968; *Savant et al.*, 1987; *Elliott and Brooks*, 1997a, 1997b]. In contrast, pool-riffle channels exhibit complex three-dimensional bed forms that span a range of partially to fully submerged conditions, inducing both static and dynamic head variations, with streambed topography having a strong effect on water-surface elevation and static pressure [e.g., *Tonina and Buffington*, 2007; 2009a, 2009b]. Bed forms in pool-riffle channels are only fully submerged during flood events. Hence, these channels exhibit transitional conditions of streambed pressure and hyporheic flow compared to previous studies of fully submerged, two-dimensional bed forms.

[7] Field studies have examined hyporheic exchange in gravel pool-riffle channels characterized by three-dimensional bed forms [e.g., *Kasahara and Wondzell,* 2003; *Storey et al.*, 2003; *Cardenas et al.*, 2004]. However, these analyses frequently employ two-dimensional simplifications. For example, *Storey et al.* [2003] analyzed the effect of hydraulic conductivity and aquifer gradient, but pool-riffle pairs were treated as two-dimensional features. Similarly, *Saenger et al.* [2005] studied the effects of stream discharge on surface-subsurface exchange, modeling pool-riffle morphology as two-dimensional bed forms. *Cardenas et al.* [2004] investigated the effects of sediment heterogeneity and river sinuosity on hyporheic flow using a three-dimensional groundwater numerical model but employed an idealized pressure distribution derived from two-dimensional bed forms, which generates a different pressure pattern than three-dimensional pool-riffle topography [*Tonina and Buffington*, 2007; *Marzadri et al.*, 2010]. Consequently, the effects of the above physical characteristics on hyporheic flow in pool-riffle channels have not been fully analyzed in a three-dimensional domain for both the surface and subsurface flow, and the effect of bed form submergence has only received limited evaluation [e.g., *Tonina and Buffington*, 2007].

[8] To address the above issues, we conduct a series of three-dimensional simulations to examine the effects of bar amplitude, stream discharge and alluvium depth on the magnitude, extent, and residence time of hyporheic flow in gravel bed rivers, with partially to entirely submerged pool-riffle morphology. Hyporheic flow is predicted from a three-dimensional pumping exchange model [*Tonina and Buffington*, 2007], with boundary conditions of channel morphology and streambed pressure based on a set of prior flume experiments [*Tonina and Buffington*, 2007]. We also apply the results of our current analysis to formulate physically based predictions of the mean exchange depth and values of the hyporheic residence time (mean and standard deviation).

2. Methods

[9] We used near-bed pressure distributions measured in a set of flume experiments with pool-riffle morphology to define the boundary conditions for the hyporheic flow model [*Tonina and Buffington*, 2007]. The model is a three-dimensional groundwater simulation based on Darcy's law.

2.1. Boundary Conditions at the Sediment Interface

[10] The flume experiments conducted by *Tonina and Buffington* [2007] provide the boundary conditions at the sediment interface for the groundwater model used in the current analysis. *Tonina and Buffington* [2007] measured the water surface elevation and the pressure distribution at the sediment interface for a set of pool-riffle morphologies with a constant bed form wavelength ($\lambda = 5.52$ m) and four amplitudes ($\Delta = 12$, 9, 6 and 3.6 cm, identified as large, medium, low, and small amplitude) for three discharges (12.5, 21, and 32.5 l s^{-1}), with two bed slopes (s = 0.0041 m m^{-1} for the two lowest discharges, and 0.0018 m m^{-1} for the highest discharge) (Table 1). In the flume experiments, only the small-amplitude bed forms were fully submerged by the flow, with the degree of submergence providing important controls on the near-bed pressure distribution and resultant hyporheic flow [*Tonina and Buffington*, 2007]. Further information about the experiments can be found in the work of *Tonina and Buffington* [2007].

2.2. Groundwater Simulations

[11] A finite volume model, FLUENT (Fluent Inc.), was used to model the hyporheic flow with Darcy's law, which describes flow through porous media when the flow has low Reynolds numbers and convective accelerations are negligible [*Dagan*, 1979], conditions that generally hold for the data used in this analysis [*Tonina and Buffington*, 2007; paragraphs 56–57]. In this case, the flow field can be evaluated by solving the Laplace equation in a three-dimensional domain

$$\nabla^2 h = 0, \tag{1}$$

coupled with Darcy's law $q = k\,\nabla h$, where h is the piezometric head, k is the sediment hydraulic conductivity, which is set equal to 0.05 m s^{-1} [*Tonina and Buffington*, 2007] and q is the hyporheic velocity. We chose a 3 cm hexahedral mesh size for our numerical simulations that was small enough to obtain a good resolution of the flow field, but large enough to satisfy Darcy's averaging of the microscopic quantities of the porous medium, and that provided mesh-independent results [*Tonina and Buffington*, 2007].

[12] The numerical domain used in the current analysis represents hyporheic flow across the channel bed only, and does not include exchange across the channel banks

Table 1. Experimental Conditions of *Tonina and Buffington* [2007], With Sediment Porosity Equal 0.34 and Hydraulic Conductivity of 0.05 m s^{-1}

	Volume of Water (m^3)	Bed Form Amplitude (Pool Bottom to Riffle Crest) (m)	Mean Water Depth (m)	Mean Wetted Width (m)	Mean Velocity (m s^{-1})	Slope (m m^{-1})	Discharge (l s^{-1})
			Large Amplitude				
Test 1	3.3	0.12	0.065	0.68	0.282	0.0041	12.5
Test 2	3.4	0.12	0.075	0.73	0.384	0.0041	21
Test 3	3.8	0.12	0.104	0.85	0.369	0.0018	32.5
			Medium Amplitude				
Test 4	3.1	0.09	0.056	0.73	0.308	0.0041	12.5
Test 5	3.2	0.09	0.064	0.79	0.413	0.0041	20.83
Test 6	3.7	0.09	0.087	0.89	0.421	0.0018	32.5
			Low Amplitude				
Test 7	2.8	0.06	0.044	0.77	0.365	0.0041	12.5
Test 8	2.9	0.06	0.053	0.87	0.46	0.0041	21.1
Test 9	3.5	0.06	0.086	0.9	0.425	0.0018	32.83
			Small Amplitude				
Test 10	3	0.036	0.039	0.9	0.367	0.0041	12.93
Test 11	3.1	0.036	0.052	0.9	0.452	0.0041	21.17
Test 12	3.4	0.036	0.082	0.9	0.442	0.0018	32.58

because those boundary conditions were not available from the flume experiments conducted by *Tonina and Buffington* [2007]. Consequently, our analyses characterize confined rivers that have little to no floodplain [*Montgomery and Buffington*, 1997]. The numerical domain spans one bed form wavelength (pool-to-pool), with dimensions identical to those used in the flume experiments of *Tonina and Buffington* [2007] (0.9 m wide by 5.5 m long), and includes seven boundaries (Figure 1). The channel walls, the base of the alluvium (e.g., bedrock in a natural channel), and the dry parts of the bars are all treated as impervious layers. The upstream and downstream ends of the bed form are set as stationary periodic boundaries with a prescribed pressure drop. The final boundary is the sediment-river interface, with boundary conditions determined from the flume experiments of *Tonina and Buffington* [2007]. The near-bed pressure profiles measured by *Tonina and Buffington* [2007] are used in all cases, except for the small-amplitude bed forms, where hydrostatic pressures are used because near bed-pressure distributions were not available. Prior work shows that the hydrostatic pressure provides a reasonable approximation of the near-bed pressure distribution for low-amplitude bed forms [*Tonina and Buffington*, 2007].

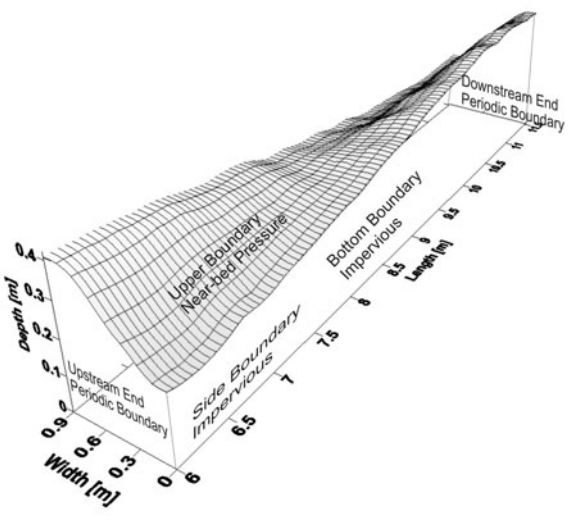

Figure 1. Numerical domain for the 0.05 λ alluvium depth and large amplitude bed form.

[13] In FLUENT, we used the pathline option for particle tracking of weightless particles that are advectively transported by the flow to estimate the residence time of the solute. At the riverbed, we numerically released 50,050 particles, and the transit time through the sediment was calculated. Moreover, we used the surface that envelopes the particle trajectories (pathlines) together with the wetted riverbed surface to define the hyporheic volume [*Tonina and Buffington*, 2007]. We use the hyporheic volume to estimate the vertical range of the hyporheic flow via the mean hyporheic depth, d_H, which we define as the total hyporheic volume divided by the wetted bathymetry of the riverbed. Particle trajectories that are entrained by the underflow and that do not re-emerge at the riverbed within our numerical domain are excluded from the hyporheic volume. The amount excluded is typically small (less than 1% of the total flux entering the riverbed surface).

[14] To analyze the effect of alluvium depth and thus the vertical position of an impervious layer, the numerical domain was created with three alluvial depths of 1 λ, 0.5 λ, and 0.05 λ, where λ is the bed form wavelength.

2.3. Residence Time Distribution

[15] The residence time distribution is defined as the cumulative probability that a tracer entering the bed at position (x, y) and at time t_0 remains in the bed longer than time t, and it is described by the relation

$$R_T(x, y, t) = \begin{cases} 1 & t \leq T \\ 0 & t > T \end{cases}, \tag{2}$$

where T is the residence time. Since the downwelling flux is a function of position (x, y, z the longitudinal, transverse,

and vertical coordinates, respectively), we weighted R_T by the local downwelling flux $q(x,y,z_b)$ (where z_b is the streambed elevation) over a representative area, defining a weighted residence time distribution (RTD). In our simulations, the flow conditions replicate themselves over each pool-riffle sequence, thus the representative surface area is that of the wetted pool-to-pool bathymetry, W_p. The RTD is calculated using the following equation:

$$\mathrm{RTD}(t) = \frac{1}{W_p\,\bar{q}} \int_0^L \int_0^{P_H(x)} q(x,y,z_b)\; R_T(t,x,y)\; dx\,dy, \qquad (3)$$

where $\bar{q}$ is the average downwelling flux over W_p, L is the length of the study reach and $P_H(x)$ is the wetted perimeter. Our model is a three-dimensional expansion of the two-dimensional framework developed by *Elliott and Brooks* [1997a, 1997b].

2.4. Solute Exchange

[16] Hyporheic mixing and solute exchange between the river and aquifer can be quantified through tracer experiments and changes in solute concentration within the channel relative to the initial value at the time of tracer injection (C/C_0). Here, we simulate the hyporheic exchange that would occur in the recirculation flume experiments of *Tonina and Buffington* [2007] over one bed form with thick alluvium (1 λ) and a spatially homogenous, instantaneous injection of solute C_0. We model the solute penetration into the streambed in terms of hyporheic advection based on the $RTD(t)$ and $\bar{q}$ [e.g., *Tonina and Buffington*, 2007]. We quantify the specific mass exchange M_e (4), which is a function of the dimensionless solute concentration, $C^* = C/C_0$, sediment porosity (ϕ), volume of water (V_w), and horizontally projected water surface area (W_s) (Table 1):

$$M_e = \frac{V_w\,(1 - C^*)}{W_s\,\phi\,C^*}. \qquad (4)$$

3. Results and Discussion

3.1. Mean Hyporheic Depth, Residence Time, Average Downwelling Flow, and Solute Exchange

3.1.1. Mean Hyporheic Depth

[17] Figure 2 shows the dimensionless mean hyporheic depth, $d_{H^*} = d_H/\lambda/\lambda$ as a function of discharge and bed form amplitude (Table 1) for three depths of alluvium and for constant hydraulic conductivity ($k = 0.05$ m s^{-1}). The figure shows that bed form amplitude and discharge affect the mean hyporheic depth for alluvial depths of 0.5–1 λ. The bed forms with the two largest amplitudes (large and medium amplitude) have the deepest hyporheic flow, which corresponds to a third of the bed form wavelength, or 2 channel widths, and occurs at low flow (12.5 l s^{-1}) when the near-bed pressure differential is largest [*Tonina and Buffington*, 2007]. Increased discharge submerges more of the bed, reducing the pressure differential and the depth of exchange. In contrast, when the bed forms are fully submerged (small amplitude), near-bed pressures increase with discharge (further discussed by *Tonina and Buffington* [2007]), causing a small increase in hyporheic depth (Figure 2). For fully submerged bed forms, the hyporheic flow

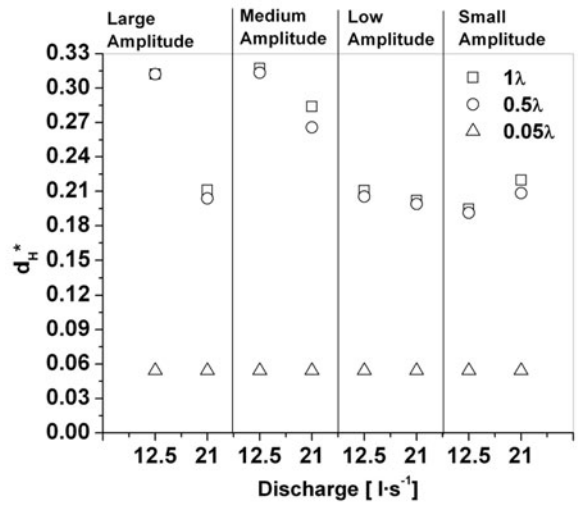

Figure 2. Dimensionless mean hyporheic depth, $d_{H^*} = d_H/\lambda$, as a function of discharge and bed form amplitude for three alluvium depths.

extends to depths of 0.2 λ, which corresponds to 1.2 channel widths; slightly greater than the analytical hyporheic depth reported by *Marzadri et al.* [2010] for fully submerged alternate-bars in equilibrium with the stream discharge. Similarly, *Cardenas and Wilson* [2007a] observed that under two-dimensional dune-like bed forms the hyporheic flow could extend vertically up to one bed form wavelength.

[18] However, when the impervious layer is shallow, the alluvium confines and determines the vertical extent of the hyporheic flow. For example, mean hyporheic depth takes a uniform value regardless of bed form amplitude for thin alluvium (0.05 λ). Therefore, thick alluvium allows the hyporheic volume to develop vertically without constraints, while thin alluvium restricts the hyporheic volume to a near-surface area. *Valett et al.* [1996] report similar results from field experiments, where hyporheic depth is unconstrained in thick alluvium, but the presence of clay lenses at 30–40 cm below the streambed effectively thin the alluvium, restricting hyporheic flows. Similarly, *Zarnetske et al.* [2008] observed that permafrost in arctic streams can confine and affect hyporheic flow. *Marzadri et al.* [2010] show that the depth of exchange is additionally influenced by stream gradient; steeper streams have faster underflow, which confines the depth of exchange to near the streambed surface.

[19] The above results indicate that the effects of discharge and bed form amplitude on hyporheic depth become negligible when the impervious layer interacts with the hyporheic flow, in which case the depth of alluvium limits the mean hyporheic depth (Figure 2). When alluvial depth is not a restriction, other factors, such as discharge and bed form amplitude, control the dimensions of the hyporheic zone. These results suggest that the hyporheic zone in pool-riffle channels is dynamic because discharge varies seasonally and in some cases daily, in pool-riffle channels [*Saenger et al.*, 2005; *Gu et al.*, 2008; *Buffington and Tonina*, 2008]. This variability imposes a certain degree of requisite adaptation for hyporheic organisms as their habitat shrinks and expands with discharge.

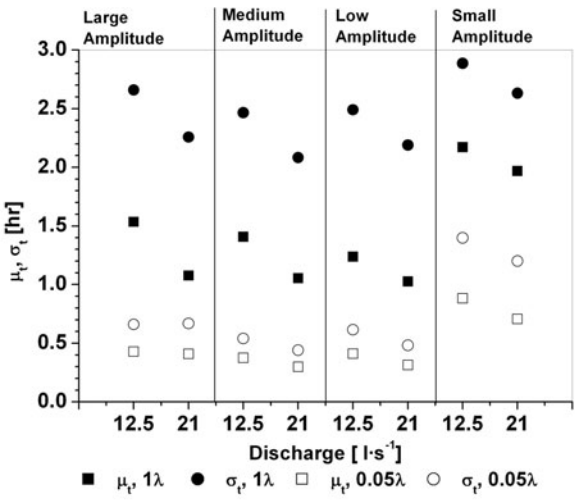

Figure 3. Mean value, μ_t, and standard deviation, σ_t, of the hyporheic residence time as functions of discharge and bed form amplitude for deep (1 λ) and thin (0.05 λ) alluvial depths.

3.1.2. Residence Time

[20] Figure 3 shows the mean (μ_t) and standard deviation (σ_t) of the hyporheic residence time distribution (RTD) for thick (1 λ) and thin (0.05 λ) alluvium. These values do not significantly change between alluvial depths of 1 λ and 0.5 λ, when the impervious layer is deeper than the hyporheic flow and, therefore, the values for 0.5 λ are not reported in Figure 3. Both μ_t and σ_t decrease with discharge for all bar amplitudes and both alluvium depths. However, the inverse relationship with discharge is less pronounced for the thin alluvium because the impervious layer compresses the hyporheic zone near the sediment interface. Moreover, for a given discharge, the mean value of RTD decreases with lower bed form amplitude up to the low-amplitude case (Figure 3), due to shallower and shorter path lines. The small amplitude boundary conditions are for fully submerged bed forms, which present lower near-bed pressure gradients than the other boundary conditions, causing higher hyporheic residence times. The decrease in mean hyporheic RTD with increasing discharge was also observed in two-dimensional numerical simulations performed by *Saenger et al.* [2005] for a pool-riffle sequence and is likely due to a reduction of near-bed pressure gradient, causing the hyporheic zone to become thinner. Similar to our results, the field observations of *Zarnetske et al.* [2008] show that hyporheic residence time distributions did not change when the impervious layer (caused by permafrost in their study) was deeper than a threshold value, all other factors being equal.

[21] The depth of alluvium has a strong impact on the time that a given amount of stream water resides in the sediment. This is particularly important for chemical reactions and biological transformations that occur within the sediment; for example, nitrification and denitrification processes need a certain amount of time to develop [*Valett et al.*, 1996; *Gu et al.*, 2007; *Cardenas et al.*, 2008a; *Pinay et al.*, 2009; *Boano et al.*, 2010]. Thus, it is important to characterize the entire hyporheic RTD.

[22] Several probability density functions for hyporheic residence time have been proposed, including exponential [*Bencala and Walters*, 1983; *Runkel*, 1998], lognormal [*Wörman et al.*, 2002; *Marzadri et al.,* 2010] and power law distributions [*Haggerty et al.,* 2002; *Cardenas et al.*, 2008b; *Bottacin-Busolin and Marion*, 2010]. In particular, *Marzadri et al.* [2010] showed that the lognormal distribution matches well the hyporheic RTD for fully submerged three-dimensional alternate-bar morphology. Here, we extend their analysis by testing if the lognormal distribution

$$\mathrm{lnorm}(t) = \frac{1}{\sqrt{2\pi\,\sigma_{\ln t}^2 t}} e^{\left[(\ln t - \mu_{\ln t})^2 / \left(2\sigma_{\ln t}^2\right)\right]}, \tag{5}$$

fits the hyporheic residence time for partially and entirely submerged bed forms, where $\mu_{\ln t}$ and $\sigma_{\ln t}$ are the mean and standard deviation of the natural log of the residence time. We also test the fit of (1) the exponential distribution

$$\exp(t) = \lambda_e e^{-\lambda_e t}, \tag{6}$$

where λ_e is the rate parameter, and (2) the power law distribution, with an exponential cut-off

$$\mathrm{powerexp}(t) = C\left(\frac{t}{t_{\min}}\right)^{\alpha} e^{-\lambda_p t}, \tag{7}$$

where C is the normalization parameter, $t_{\min}$ is a threshold value, which we set equal to the shortest residence time, and α and λ_p are distribution parameters [*Clauset et al.*, 2009]. We estimate the distribution parameters with the maximum likelihood method. This method provides the following closed form solutions for the lognormal and exponential distribution parameters:

$$\begin{aligned} \mu_{\ln t} &= \frac{1}{NP}\sum_{j=1}^{NP} \ln t_j; \;\; \sigma_{\ln t}^2 = \frac{1}{NP}\sum_{j=1}^{NP} \left(\ln t_j - \mu_{\ln t}\right)^2; \\ \lambda_e &= \left(\frac{1}{NP}\sum_{j=1}^{NP} t_j\right)^{-1} \end{aligned} \tag{8}$$

where NP is the number of upwelling particles [*Clauset et al.*, 2009]. A close form of the parameters for the power law with exponential cut off is not available, and we fit numerically the data to estimate α and λ_p using the maximum likelihood method [*Clauset et al.*, 2009].

[23] Figure 4 shows Q-Q plots comparing the fit of the above distributions to the simulated hyporheic residence times for Tests 1–12 for unconstrained hyporheic flow (depth of alluvium equal to 1 λ); the comparison is expressed in terms of cumulative distribution functions (CDFs). Results indicate that the RTD is approximately lognormal for both partially and entirely submerged pool-riffle bed forms. Similar results are obtained for the thin alluvium, but are not reported here. Our findings agree with previous studies, which indicate that hyporheic flows induced by two- and three-dimensional topography have lognormal RTDs [*Wörman et al.*, 2002; *Cardenas et al.*, 2004; *Marzadri et al.*, 2010], with our results extending the use of the lognormal model to both entirely and partially submerged pool-riffle topography.

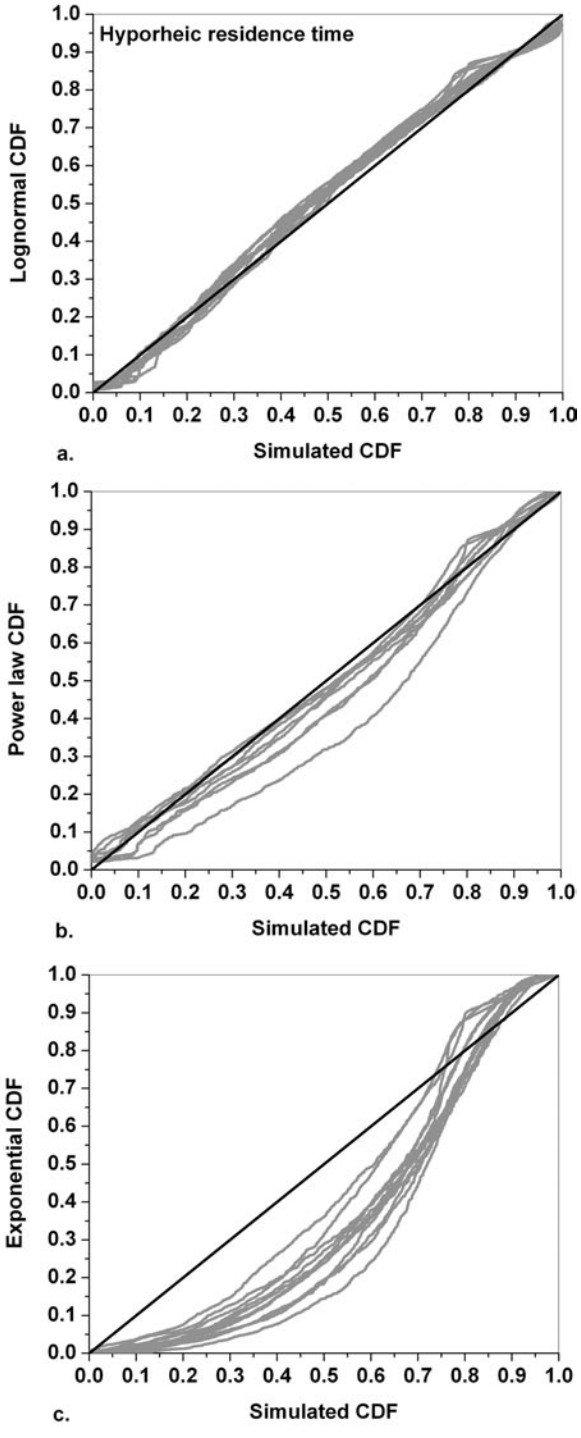

Figure 4. Q-Q plot of the hyporheic residence time for 1 λ alluvium depth, comparing the simulated cumulative distribution functions (CDF) of Tests 1–12 with (a) lognormal (b) power law with exponential cutoff and (c) exponential distributions.

[24] When calculating the mean residence time, we did not consider particles entrained by the underflow because those particles do not return to the surface within the modeling domain and are, therefore, not part of the hyporheic exchange, *sensu stricto*. However, if we had considered all the injected particles when evaluating the residence time distribution, we would have observed that the mean residence time would have varied with the length of the simulations. In the model, the pathlines of the particles entrained into the underflow are of infinite length since they do not return to the riverbed surface. The partial loss of solute to the underflow also happens in real rivers (e.g., in losing reaches or due to streambed irregularities), in which case the mean residence time is a less valuable measure because it is a function of experiment length. In contrast, the median residence time is not influenced by the small number of particles lost to the underflow and may be a more suitable metric for hyporheic flow in field experiments. Note that the median of the residence time, t_{50}, relates to the mean of the natural log of the residence time $\mu_{\ln t}$ with the following equation

$$t_{50} = e^{\mu_{\ln t}}, \tag{9}$$

for a lognormally distributed residence time distribution; a form that is supported both by this work and previous studies examining bed form-induced exchange [e.g., *Wörman et al.*, 2002; *Cardenas et al.*, 2004; *Marzadri et al.*, 2010].

3.1.3. Average Downwelling Flow

[25] Thin alluvium presents less downwelling flux than deeper alluvium (Figure 5) because smaller volumes of sediment are available for developing hyporheic flow. The change in flux is negligible between 1 λ and 0.5 λ because the impervious layer is deeper than the hyporheic flow (Table 2). However, there is a 12%–29% decrease in average downwelling flux when the depth of alluvium is reduced from 0.5 λ to 0.05 λ, limiting the depth of hyporheic exchange (Table 2). In contrast, *Storey et al.* [2003] reported that the depth of alluvium does not affect hyporheic exchange flux. Our results show that this is true for thick alluvium that extends below the hyporheic zone, which is the case *Storey et al.* [2003] analyzed, but that thin alluvium can affect the exchange flux when it interacts with and limits hyporheic flow. This effect has also been

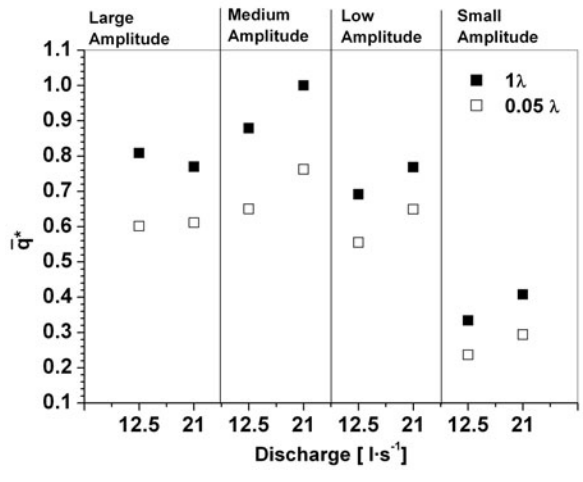

Figure 5. Dimensionless mean downwelling flux $\bar{q}^* = \bar{q}/\bar{q}_{\max}$ where $\bar{q}_{\max}$ is the largest predicted mean downwelling flux (Test 5, 1 λ) as a function of discharge and bed form amplitude for homogeneous alluvium with depths of 1 λ and 0.05 λ.

Table 2. Percentage Change in Average Downwelling Flux, $\bar{q}$, as a Function of Alluvium Thickness Scaled by Bed Form Wavelength (λ)

	Downwelling Flux, 0.5 λ to 0.05 λ
Test 1	−25.66%
Test 2	−20.62%
Test 3	−17.61%
Test 4	−26.04%
Test 5	−23.80%
Test 6	−18.31%
Test 7	−19.77%
Test 8	−15.55%
Test 9	−11.93%
Test 10	−29.05%
Test 11	−27.92%
Test 12	−17.91%

[a] $\bar{q}$ does not change significantly between 1 λ to 0.5 λ.

show for two-dimensional bed forms [*Wörman et al.*, 2002; *Cardenas and Wilson*, 2007a]. Furthermore, Figure 5 shows that stream discharge influences hyporheic flux both for thick and thin alluvium. The downwelling flux generally increases with discharge, as also observed by *Saenger et al.* [2005]. This finding differs from that reported by *Storey et al.* [2003] because of their erroneous approach of simulating different flow stages by adding uniform layers of flow depth and stream head, thus maintaining the same head gradients. For partially submerged topography, local stream heads fall and rise differently with discharge depending on their position in the stream [e.g., *Tonina and Buffington*, 2007], and this change in pressure pattern with discharge influences the downwelling flux, making stream stage a key factor in studying hyporheic flow in such channels. Local topographic steering also becomes an important factor at low discharge.

3.1.4. Solute Exchange

[26] Figure 6 shows the effective depth of penetration, M_e, as a function of time, bed from amplitude and discharge for thick alluvium (1 λ). The fastest exchange rate occurs for the medium-amplitude bed form (Figure 6, $\Delta =$ 9 cm). The medium-amplitude bed form also shows a larger final value of M_e, indicating greater total exchange. This bed form amplitude has the most effective combination of downwelling flux and mean hyporheic depth (analyzed in previous sections).

[27] An increase of river discharge results in a lower initial hyporheic exchange rate (e.g., cf. Figure 6a–6b, $\Delta =$ 12 cm), which is caused by a reduction in pressure gradient for the larger amplitude bed forms (large, medium, and low amplitude) due to smoothing of the water surface profile with bed form submergence, as discussed earlier [*Tonina and Buffington*, 2007]. The difference in surface-subsurface exchange between discharges diminishes with lower bed form amplitude, becoming negligible for the lowest amplitude case (Figure 6, $\Delta = 3.6$ cm).

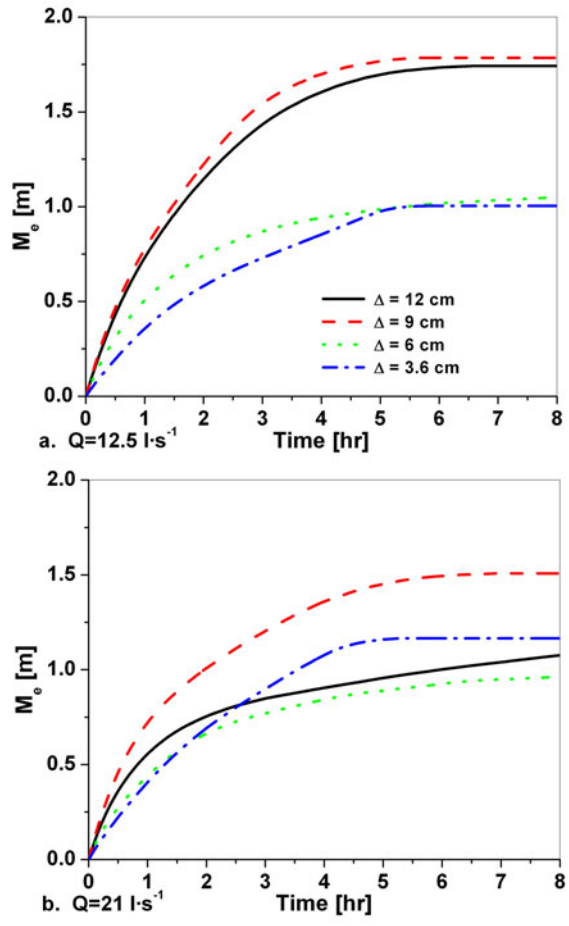

Figure 6. Hyporheic solute exchange, expressed in terms of the effective depth of penetration M_e, as a function of bed form amplitude (Δ) and (a) low and (b) medium discharges for 1 λ thick homogeneous alluvium.

3.2. Flowpaths

[28] We used pathlines to visualize the hyporheic flow inside the porous medium for two depths of alluvium: (1) thick (Figure 7a) and (2) thin (Figure 7b).

[29] For thick alluvium, the hyporheic flow is complex (Figure 7a). There is a near-surface zone where the flow paths cross the riffle crest from one side to the other of the river. This motion follows the surface water flow. Deeper flows present trajectories more inline with the longitudinal axis of the river than shallower flows, creating a deep hyporheic flow cell. They span the pool-riffle unit and have three-dimensional behavior close to the surface, where low-pressure areas redirect them. This highlights the effect of local topography on river-groundwater interaction [*Harvey and Bencala*, 1993; *Woessner*, 2000; *Cardenas et al.*, 2004]. Local topography via high- and low-pressure areas determines where groundwater can enter the river and where river water can recharge the aquifer [*Harvey and Bencala*, 1993; *Woessner*, 2000].

[30] In contrast, when the alluvium is thin, the hyporheic flow is correspondingly shallow, but three-dimensional, again, with intense flux at the crest of the riffle (Figure 7b). There are several strong downwelling areas: at the middle of the stoss side of the riffle, and at the upstream end of the bar. Strong upwelling areas are located at the middle of the lee side of the riffle and at the pool head, close to the bar side.

[31] The fisheries literature indicates that salmonid nests (redds) are typically built in upwelling and downwelling areas [*Geist and Dauble,* 1998; *Baxter and Hauer*, 2000]. For example, salmonids commonly spawn in pool tails,

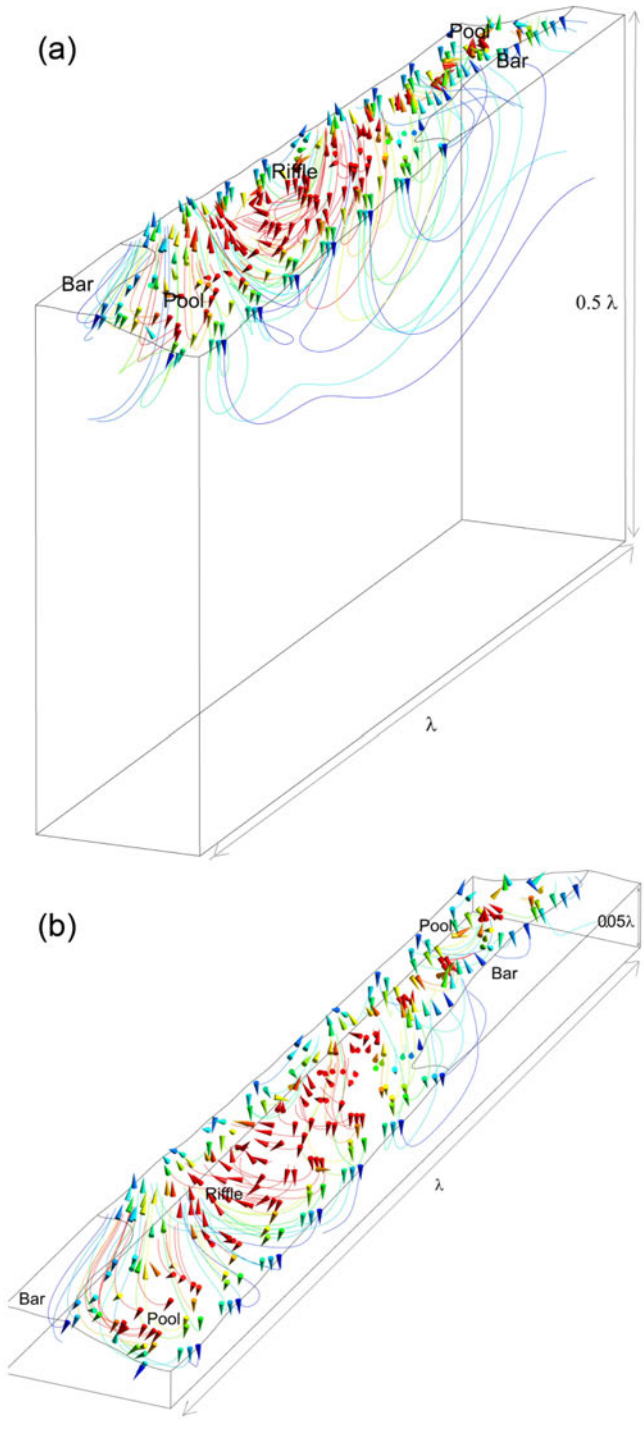

Figure 7. Pathlines colored by particle ID for pool-riffle morphology Test 2 (large amplitude and medium discharge), (a) homogeneous alluvium with a depth of 0.5 λ, (b) homogeneous alluvium with a depth of 0.05 λ.

which are hydraulic transitional zones upstream of the riffle, where in-stream water accelerates and downwelling fluxes are present [*Stuart*, 1953; *Hoopes,* 1972; *Vronskiy*, 1972]. When they spawn downstream of the riffle, it is close to the gravel bar side, where the current is less intense than over the riffle (R. Thurow, personal communication, 2004). Figure 7 shows abundant upwelling fluxes in this area. Areas with intense upwelling and downwelling, around the two bar ends and at the two sides of the riffle, might offer strong hyporheic fluxes with short residence times that will preserve oxygen concentrations and provide a more appealing environment for spawning, and greater potential for successful incubation of salmon eggs [e.g., *Greig et al.*, 2007].

3.3. Predicting Mean Hyporheic Depth and Residence Time

[32] We used our findings to develop empirical equations for predicting the mean depth of exchange and characteristic values of the residence time distribution (mean and standard deviation). The mean residence time combined with the average hyporheic depth represents the retention of the hyporheic zone. Thus, empirical predictions of these values would quantify first-order approximations of the extent and retention of the hyporheic zone without numerical modeling.

3.3.1. Mean Hyporheic Depth

[33] We assumed that the mean hyporheic depth, d_H, is a function of mean flow velocity, v, average water depth, d, water density, ρ, dynamic viscosity of the water, μ, gravity, g, bed slope, s, alluvial depth d_a, permeability of the alluvium, K, bed form amplitude, Δ, and bed form wavelength, λ.

[34] Furthermore, the hyporheic depth is meaningful only if it is shallower than the impervious layer (alluvium depth), which would otherwise constrain and define the hyporheic depth. Consequently, K and d_a are dropped from our prediction of mean hyporheic depth, assuming that $d_a > d_H$.

[35] To reduce the number of variables, we applied the Buckingham π theorem by using mean flow velocity, water density, and mean water depth as governing variables. This operation simplifies the problem from nine variables to five dimensionless groups, which are Reynolds number, Re, Froude number, Fr, bed slope, the ratio of bed form amplitude to water depth, and the ratio of bed form wavelength to water depth

$$\Pi_1' = \frac{\rho v d}{\mu}; \quad \Pi_2' = \frac{v}{\sqrt{g d}}; \quad \Pi_3' = \frac{\Delta}{d}; \quad \Pi_4' = \frac{\lambda}{d}; \quad \Pi_5' = s; \quad (10)$$

$$\frac{d_H}{d} = \exp\left[\sum_{i=1}^{5} A_i \ln\left(\Pi_i'\right)\right]. \quad (11)$$

[36] We performed a linear regression analysis on the natural log of the dimensionless numbers to determine the five coefficients, A_i, of equation (8) (Table 3). The predicted values show good agreement with the simulated quantities (Figure 8, with a zero intercept imposed for the regression line).

3.3.2. Mean and Standard Deviation of the Hyporheic Residence Time

[37] The permeability and depth of alluvium are key factors in evaluating the hyporheic residence time; consequently, we use the simulation results for all alluvial depths (i.e., both vertically constrained and unconstrained hyporheic zones). In applying the Buckingham π theorem, we defined a new set of governing variables: the mean flow velocity, water density, and hydraulic permeability. We attained the following nondimensional numbers:

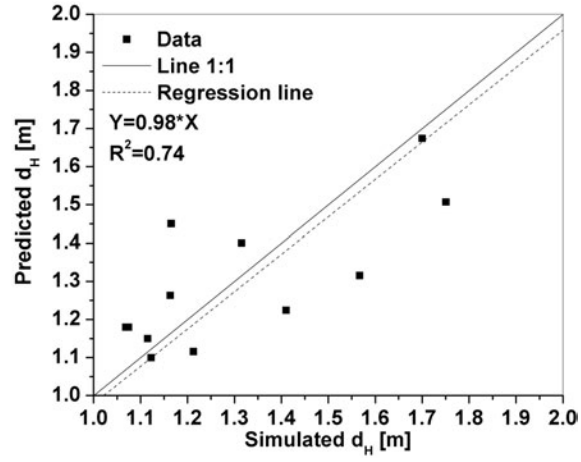

Figure 8. Simulated versus predicted (equation (11)) mean hyporheic depth.

$$\Pi_1 = \frac{\rho v \sqrt{K}}{\mu}; \quad \Pi_2 = \frac{v^2}{g\sqrt{K}}; \quad \Pi_3 = \frac{d}{\sqrt{K}};$$
$$\Pi_4 = s; \quad \Pi_5 = \frac{\Delta}{\lambda}; \quad \Pi_6 = \frac{d_a}{\sqrt{K}}. \quad (12)$$

The above dimensionless parameters were used to estimate the mean (μ_t) and standard (σ_t) deviation of the hyporheic residence time using the following expressions:

$$\frac{\mu_t v}{\sqrt{K}} = \exp\left[\sum_{i=1}^{6} B_i \ln(\Pi_i)\right] \quad (13)$$

$$\frac{\sigma_t v}{\sqrt{K}} = \exp\left[\sum_{i=1}^{6} B_i' \ln(\Pi_i)\right]. \quad (14)$$

[38] A linear regression procedure of the logged values similar to the one described in the previous section was used to determine the six coefficients, B_i, and B_i' (Table 3). Predicted values show good agreement with the simulated quantities (Figure 9).

[39] These relationships can provide first-order approximations for laterally confined rivers with homogeneous and isotropic alluvium. Such streams are typically located in canyons with little to no floodplain [*Montgomery and Buffington*, 1997], and may present predominantly longitudinal exchange and limited lateral connection with the floodplain [e.g., *Buffington and Tonina*, 2009; *Tonina and Buffington*, 2009a]. The variables used in equations (11), (13), and (14)

Table 3. Empirically Determined Parameters for Equations (11), (13) and (14)

i		1	2	3	4	5	6
Hyporheic mean depth (11)	A_i	0.152	−0.058	−0.509	0.074	0.906	
Mean hyporheic residence time (13)	B_i	−0.682	0.387	1.619	0.314	−1.339	0.407
Hyporheic residence time SD (14)	B_i'	−0.533	0.652	1.369	0.098	−1.066	0.456

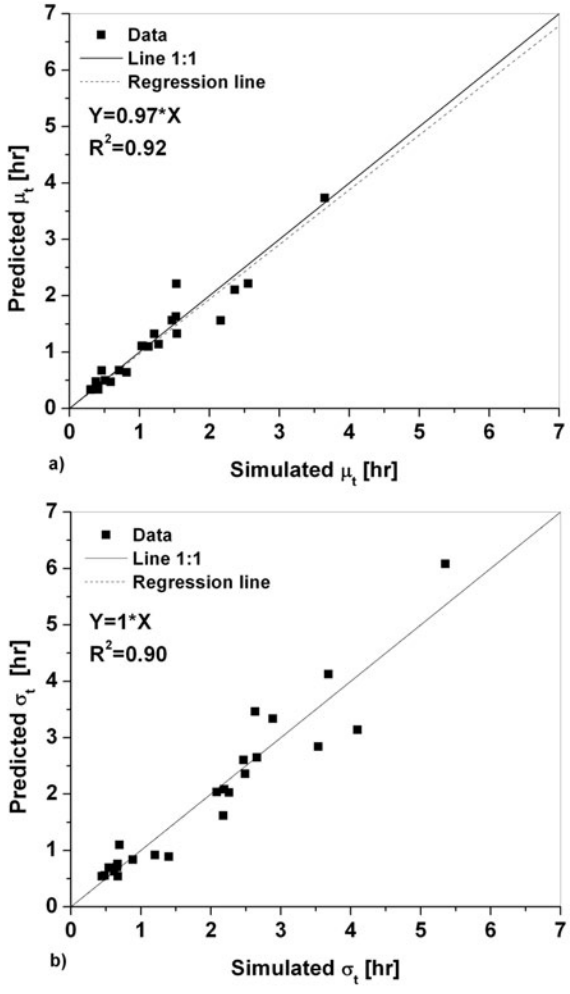

Figure 9. Simulated versus predicted (a) mean hyporheic residence time (equation (13)) and (b) standard deviation of the hyporheic residence time (equation (14)).

can be estimated in the field and are used in other hyporheic flow models [*Elliott and Brooks*, 1997a; *Marzadri et al.*, 2010]. For instance, K can be expressed as a function of grain size distribution [*Das*, 1998] or in situ permeability tests [e.g., *Baxter and Hauer*, 2000], while v can be determined from dye tracers. Relationship (11) can be used to assess the vertical extent of the hyporheic zone and hence of the interaction between the river and its streambed sediment [e.g., *Smith*, 2005]. Equation (13) can provide the retention capacity of the hyporheic zone and suggest whether aerobic or anaerobic conditions most likely occur in the hyporheic zone [e.g., *Triska et al.*, 1993; *Sheibley et al.*, 2003; *Buss et al.*, 2005; *Cardenas et al.*, 2008a]. Small values of μ_t would indicate prevailing aerobic conditions, which support nitrification and other oxidizing reactions within the hyporheic zone. Conversely, large values of μ_t suggest prevalent anaerobic conditions and thus reducing reactions (e.g., denitrification). Additionally, equations (13) and (14) can be used to estimate the parameters for the lognormal distribution, which would provide the complete hyporheic residence time distribution. Equations (11), (13), and (14) are not appropriate for unconfined floodplain rivers, where stream sinuosity generates hyporheic flow across meander bends and through the floodplain [*Cardenas et al.*, 2004; *Boano et al.*, 2006; *Boano et al.*, 2008; *Buffington and Tonina*, 2009; *Cardenas*, 2009; *Tonina and Buffington*, 2009a].

4. Conclusion

[40] Topographically induced hyporheic flow is an important mechanism that exchanges solutes between streams and their underlying sediment, maintaining aerobic environments within portions of the streambed. Many factors are involved in hyporheic exchange, including stream discharge, bed form amplitude, and depth of alluvium. We investigated the importance of these factors in controlling the hyporheic residence time distribution, downwelling flux, and depth of hyporheic exchange and summarize our results in Table 4.

[41] Stream discharge is a significant factor because it controls the pressure distribution at the sediment interface, and it remains important for different combinations of all the other factors [*Saenger et al.*, 2005]. Bed form amplitude provides significant control on channel hydraulics and hyporheic exchange. The depth of alluvium is not a controlling factor for hyporheic exchange as long as it is deeper than the hyporheic flow paths, which in our simulations correspond to depths of 0.3 λ (one third of the pool-riffle wavelength). When the alluvium is thinner than 0.3 λ, as may be common in confined headwater channels or in arctic streams [*Zarnetske et al.*, 2008], the hyporheic flow is confined by an impervious layer (bedrock or permafrost), causing a reduction of the residence time distribution (RTD) and downwelling rates. In such channels, depth of alluvium is the primary control on the character of hyporheic flow.

[42] The location and extent of upwelling and downwelling is primarily controlled by the surface pressure distribution, not by the depth of alluvium, or hydraulic conductivity of a homogenous medium [e.g., *Harvey and Wagner*, 2000;

Table 4. Relationship Between Hyporheic Flow and Stream Discharge, Bar Amplitude, and Alluvial Depth[a]

	Stream Discharge (Q)	Bar Amplitude (Δ)	Alluvial Depth (d_a)
Mean hyporheic depth d_H	$d_H\downarrow$ as Q↑ for partially submerged topography[b]; $d_H\uparrow$ as Q↑ for entirely submerged topography	$d_H\downarrow$ as $\Delta\downarrow$ generally	$d_H\downarrow$ as $d_a\downarrow$
Mean hyporheic residence time μ_t	$\mu_t\downarrow$ as Q↑	$\mu_t\downarrow$ as D↓ for partially submerged topography	$\mu_t\downarrow$ as $d_a\downarrow$
SD of the hyporheic residence time σ_t	$\sigma_t\downarrow$ as Q↑ generally	$\sigma_t\downarrow$ as $\Delta\downarrow$ for partially submerged topography	$\sigma_t\downarrow$ as $d_a\downarrow$
Average downwelling flux $\bar{q}$	$\bar{q}\uparrow$ as Q↑ generally	$\bar{q}\uparrow$ as $\Delta\uparrow$ generally	$\bar{q}\downarrow$ as $d_a\downarrow$

[a]All info is the Lognormal distribution.
[b]Note that ↑ means increase, ↓ decrease.

Tonina and Buffington, 2009a]. These factors mainly affect either the residence time distribution or the hyporheic flux, while the spatial pattern of hyporheic flow is controlled by bed topography and channel hydraulics, the interaction of which affects the spatial variation of near-bed pressure that is responsible for locations of downwelling and upwelling flow. Our simulations show that hyporheic flow induced by partially submerged pool-riffle morphology results in a lognormally distributed residence time distribution, extending the use of the lognormal model beyond its prior application to two-dimensional bed forms and fully submerged alternate bars [*Wörman et al.*, 2002; *Cardenas et al.*, 2004; *Marzadri et al.*, 2010].

[43] We also developed an empirical relationship to predict the mean hyporheic depth and mean and standard deviation of the residence time based on stream discharge, channel geometry and substrate characteristics. These relationships can be used in confined rivers with homogeneous and isotropic alluvium. Equations (13) and (14) can be used to estimate the parameters for the lognormal distribution to evaluate the entire hyporheic residence time distribution. Further studies are necessary to evaluate the importance of these factors for different bed form wavelengths in unconfined floodplain rivers. In our work, we changed the amplitude, but kept the wavelength constant. Deeper pools and shorter wavelengths are common in many Pacific Northwest gravel bed rivers where pool-riffle topography is forced by frequent wood obstructions [e.g., *Montgomery et al.*, 1995; *Collins and Montgomery*, 2002; *Buffington et al.*, 2002], and may show different behavior than those presented herein [e.g., *Lautz et al.*, 2006; *Mutz et al.*, 2007].

[44] **Acknowledgments.** This work was supported in part by the STC Program of the National Science Foundation under Agreement Number EAR-0120914, the USDA Forest Service, Yankee Fork Ranger District (00-PA-11041303-071), and by Congressional Award: Fund for the Improvement of Post2ndary Education (Award Number P116Z010107) Advanced Computing and Modeling Laboratory at the University of ID. Comments from Alberto Bellin, Peter Goodwin, Klaus Jorde, three anonymous reviewers and the associate editor improved the manuscript.

References

Baxter, C. V., and R. F. Hauer (2000), Geomorphology, hyporheic exchange, and selection of spawning habitat by bull trout (*Salvelinus confluentus*), *Can. J. Fish. Aquat. Sci.*, *57*, 1470–1481.

Bencala, K. E., and R. A. Walters (1983), Simulation of solute transport in a mountain pool-and-riffle stream: A transient storage model, *Water Resour. Res.*, *19*(3), 718–724, doi:10.1029/WR019i003p00718.

Boano, F., C. Camporeale, R. Revelli, and L. Ridolfi (2006), Sinuosity-driven hyporheic exchange in meandering rivers, *Geophys. Res. Lett.*, *33*, L18406, doi:10.1029/2006GL027630.

Boano, F., R. Revelli, and L. Ridolfi (2008), Reduction of the hyporheic zone volume due to the stream-aquifer interaction, *Geophys. Res. Lett.*, *35*, L09401, doi:10.1029/2008GL033554.

Boano, F., A. Demaria, R. Revelli, and L. Ridolfi (2010), Biogeochemical zonation due to intrameander hyporheic flow, *Water Resour. Res.*, *46*, W02511, doi:10.1029/2008WR007583.

Bottacin-Busolin, A., and A. Marion (2010), Combined role of advective pumping and mechanical dispersion on time scales of bed form-induced hyporheic exchange, *Water Resour. Res.*, *46*, W08518, doi:10.1029/2009WR008892.

Boulton, A. J., S. Findlay, P. Marmonier, E. H. Stanley, and M. H. Valett (1998), The functional significance of the hyporheic zone in streams and rivers, *Ann. Rev. Ecol. Syst.*, *29*, 59–81.

Brunke, M., and T. Gonser (1997), The ecological significance of exchange processes between rivers and groundwater, *Freshwater Biol.*, *37*, 1–33.

Buffington, J. M., and D. R. Montgomery (1999a), A procedure for classifying textural facies in gravel-bed rivers, *Water Resour. Res.*, *35*(6), 1903–1914, doi:10.1029/1999WR900041.

Buffington, J. M., and D. R. Montgomery (1999b), Effects of hydraulic roughness on surface textures of gravel-bed rivers, *Water Resour. Res.*, *35*(11), 3507–3522, doi:10.1029/2000WR900412.

Buffington, J. M., and D. Tonina (2008), Discussion of "Evaluating vertical velocities between the stream and the hyporheic zone from temperature data" by I. Seydell, B. E. Wawra, and U. C. E. Zanke, in *Gravel-Bed Rivers 6-From Process Understanding to River Restoration*, edited by H. Habersack et al., pp. 128–131, Elsevier, Amsterdam, Netherlands.

Buffington, J. M., and D. Tonina (2009), Hyporheic exchange in mountain rivers II: Effects of channel morphology on mechanics, scales, and rates of exchange, *Geogr. Compass*, *3*(3), 1038–1062.

Buffington, J. M., T. E. Lisle, R. D. Woodsmith, and S. Hilton (2002), Controls on the size and occurrence of pools in coarse-grained forest rivers, *River Res. Appl.*, *18*, 507–531.

Buffington, J. M., D. R. Montgomery, and H. M. Greenberg (2004), Basin-scale availability of salmonid spawning gravel as influenced by channel type and hydraulic roughness in mountain catchments, *Can. J. Fish. Aquat. Sci.*, *61*, 2085–2096.

Buss, S. R., M. O. Rivett, P. Morgan, and C. D. Bemment (2005), Attenuation of nitrate in the sub-surface environment, *Sci. Rep. SC030155/SR2*, Environ. Agency, Bristol, U. K.

Clauset, A., C. R. Shalizi, and M. E. J. Newman (2009), Power-law distributions in empirical data, *SIAM Rev.*, *51*(4), 661–703.

Cardenas, M. B. (2009), Stream-aquifer interactions and hyporheic exchange in gaining and losing sinuous streams, *Water Resour. Res.*, *45*, W06429, doi:10.1029/2008WR007651.

Cardenas, M. B., and J. L. Wilson (2007a), Hydrodynamics of coupled flow above and below a sediment–water interface with triangular bedforms, *Adv. Water Resour.*, *30*, 301–313.

Cardenas, M. B., and J. L. Wilson (2007b), Exchange across a sediment–water interface with ambient groundwater discharge, *J. Hydrol.*, *346*, 69–80, doi:10.1016/j.jhydrol.2007.08.019.

Cardenas, M. B., J. L. Wilson, and V. A. Zlotnik (2004), Impact of heterogeneity, bed forms, and stream curvature on subchannel hyporheic exchange, *Water Resour. Res.*, *40*, W08307, doi:10.1029/2004WR003008.

Cardenas, M. B., P. L. M. Cook, H. Jiang, and P. Traykovski (2008a), Constraining denitrification in permeable wave-influenced marine sediment using linked hydrodynamic and biogeochemical modeling, *Earth Planet. Sci. Lett.*, *275*(1–2), 127–137, doi:10.1016/j.epsl.2008.08.016.

Cardenas, M. B., J. L. Wilson, and R. Haggerty (2008b), Residence time of bedform-driven hyporheic exchange, *Adv. Water Resour.*, *31*(10), 1382–1386, doi:10.1016/j.advwatres.2008.07.006.

Collins, B. D., D. R. Montgomery, and A. D. Haas (2002), Historical changes in the distribution and functions of large wood in Puget Lowland rivers, *Can. J. Fish. Aquat. Sci.*, *59*, 66–76.

Dagan, G. (1979), The generalization of Darcy's law for nonuniform flow, *Water Resour. Res.*, *15*(1), 1–7, doi:10.1029/WR015i001p00001.

Dahm, C. N., M. H. Valett, C. V. Baxter, and W. W. Woessner (2006), Hyporheic Zones, in *Methods in Stream Ecology*, edited by F. R. Hauer and G. A. Lamberti, pgs. 119–142, Elsevier, London, U.K.

Das, M. B. (1998), *Principles of Geotechnical Engineering*, PWS Publ., Boston, Mass.

Doering, M., U. Uehlinger, A. Rotach, D. R. Schlaepfer, and K. Tockner (2007), Ecosystem expansion and contraction dynamics along a large Alpine alluvial corridor (Tagliamento River, Northeast Italy), *Earth Surf. Processes Landforms*, *32*, 1693–1704.

Edwards, R. T., (1998), The hyporheic zone, in *River Ecology and Management: Lessons from the Pacific Coastal Ecoregion*, edited by R. J. Naiman and R. E. Bilby, pp. 399–429, Springer, New York.

Elliott, A. H., and N. H. Brooks (1997a), Transfer of nonsorbing solutes to a streambed with bed forms: Laboratory experiments, *Water Resour. Res.*, *33*(1), 137–151, doi:10.1029/96WR02783.

Elliott, A. H., and N. H. Brooks (1997b), Transfer of nonsorbing solutes to a streambed with bed forms: Theory, *Water Resour. Res.*, *33*(1), 123–136, doi:10.1029/96WR02784.

Geist, D. R., and D. D. Dauble (1998), Redd site selection and spawning habitat use by fall Chinook salmon: the importance of geomorphic features in large rivers, *Environ. Manage.*, *22*(5), 655–669.

Gooseff, M. N., J. K. Anderson, S. M. Wondzell, J. LaNier, and R. Haggerty (2005), A modelling study of hyporheic exchange pattern and the sequence, size, and spacing of stream bedforms in mountain stream networks, Oregon, USA, *Hydrol. Processes*, *19*, 2915–2929.

Greig, S. M., D. A. Sear, and P. A. Carling (2007), A review of factors influencing the availability of dissolved oxygen to incubating salmonid embryos, *Hydrol. Proc.*, *21*, 323–334, doi:10.1002/hyp.6188.

Grimm, N. B., and S. G. Fisher (1984), Exchange between interstitial and surface water: Implication for stream metabolism and nutrient cycling, *Hydrobiologia*, *111*, 219–228.

Gu, C., G. M. Hornberger, A. L. Mills, J. S. Herman, and S. A. Flewelling (2007), Nitrate reduction in streambed sediments: Effects of flow and biogeochemical kinetics, *Water Resour. Res.*, *43*, W12413, doi:10.1029/2007WR006027.

Gu, C., G. M. Hornberger, J. Herman, and A. Mills (2008), Effect of freshets on the flux of groundwater nitrate through streambed sediments, *Water Resour. Res.*, *44*, W05415, doi:10.1029/2007WR006488.

Haggerty, R., S. M. Wondzell, and M. A. Johnson (2002), Power-law residence time distribution in hyporheic zone of a 2nd-order mountain stream, *Geophys. Res. Lett.*, *29*(13), 1640, 4, doi:10.1029/2002GL014743.

Harvey, J. W., and K. E. Bencala (1993), The effect of streambed topography on surface-subsurface water exchange in mountain catchments, *Water Resour. Res.*, *29*, 89–98, doi:10.1029/92WR01960.

Harvey, J. W., and B. J. Wagner (2000), Quantifying hydrologic interactions between streams and their subsurface hyporheic zones, in *Streams and Ground Waters*, edited by J. B. Jones and P. J. Mulholland, pp. 3–44, Academic, San Diego, Calif.

Hassanizadeh, M. S., and W. G. Gray (1979), General conservation equations for multi-phase systems: 1. Averaging procedure, *Adv. Water Resour.*, *2*, 131–144.

Hill, A. R. (2000), Stream chemistry and riparian zones, in *Streams and Ground Waters*, edited by J. B. Jones and P. J. Mulholland, pp. 83–110, Academic, San Diego, Calif.

Hill, A. R., and J. Lymburner (1998), Hyporheic zone chemistry and stream-subsurface exchange in two groundwater-fed streams, *Can. J. Fish. Aquat. Sci.*, *55*, 495–506.

Hoopes, D. T. (1972), Selection of spawning sites by sockeye salmon in small streams, *Fish. Bull.*, *70*(2), 447–457.

Jones, J. B., and P. J. Mulholland (Eds.) (2000), *Streams and Ground Waters*, 425 pp., Academic, San Diego, Calif.

Jones, K. L., G. C. Poole, W. W. Woessner, M. V. Vitale, B. R. Boer, S. J. O'Daniel, S. A. Thomas, and B. A. Geffen (2007), Geomorphology, hydrology, and aquatic vegetation drive seasonal hyporheic flow patterns across a gravel-dominated floodplain, *Hydrol. Processes*, *22*, 2105–2113.

Kasahara, T., and S. M. Wondzell (2003), Geomorphic controls on hyporheic exchange flow in mountain streams, *Water Resour. Res.*, *39*(1), 1005, doi:10.1029/2002WR001386.

Lautz, L. K., D. I. Siegel, and R. L. Bauer (2006), Impact of debris dams on hyporheic interaction along a semi-arid stream, *Hydrol. Proc.*, *20*, 183–196.

Lisle, T. E., and S. Hilton (1992), The volume of fine sediment in pools: an index of sediment supply in gravel-bed streams, *Water Resour. Bull.*, *28*(2), 371–382.

Malard, F., K. Tockner, M.-J. Dole-Olivier, and J. V. Ward (2002), A landscape perspective of surface–subsurface hydrological exchanges in river corridors, *Freshwater Biology*, *47*, 621–640.

Maridet, L., J. G. Wasson, and M. Philippe (1992), Vertical distribution of fauna in the bed sediment of three running water sites: influence of physical and trophic factors, *Reg. Rivers: Res. Mgmt.*, *7*, 45–55.

Marion, A., M. Bellinello, I. Guymer, and A. I. Packman (2002), Effect of bed form geometry on the penetration of nonreactive solutes into a streambed, *Water Resour. Res.*, *38*(10), 1209, doi:10.1029/2001WR000264.

Marzadri, A., D. Tonina, A. Bellin, and G. Vignoli (2010), Effects of bar topography on hyporheic flow in gravel-bed rivers, *Water Resour. Res.*, *46*, W07531, doi:10.1029/2009WR008285.

Montgomery, D. R., and J. M. Buffington (1997), Channel-reach morphology in mountain drainage basins, *Geol. Soc. Am. Bull.*, *109*, 596–611.

Montgomery, D. R., J. M. Buffington, R. D. Smith, K. M. Schmidt, and G. Pess (1995), Pool spacing in forest channels, *Water Resour. Res.*, *31*, 1097–1105, doi:10.1029/94WR03285.

Mutz, M., E. Kalbus, and S. Meinecke (2007), Effect of instream wood on vertical water flux in low-energy sand bed flume experiments, *Water Resour. Res.*, *43*, W10424, doi:10.1029/2006WR005676.

Naiman, R. J. (1998), Biotic stream classification, in *River Ecology and Management: Lessons from the Pacific Coastal Ecoregion*, edited by R. J. Naiman and R. E. Bilby, pp. 97–119, Springer, New York.

NRC (2002), *Riparian Areas: Functions and Strategies for Management*, 428 pp., Natl. Acad. Press, Washington, D. C.

Packman, A. I., N. H. Brooks, and J. J. Morgan (2000), A physicochemical model for colloid exchange between a stream and a sand streambed with bed forms, *Water Resour. Res.*, *36*(8), 2351–2361, doi:10.1029/2000WR900059.

Packman, A. I., M. Salehin, and M. Zaramella (2004), Hyporheic exchange with gravel beds: basic hydrodynamic interactions and bedform-induced advective flows, *J. Hydraul. Eng.*, *130*(7), 647–656.

Pinay, G., T. C. O'Keefe, R. T. Edwards, and R. J. Naiman (2009), Nitrate removal in the hyporheic zone of a salmon river in Alaska, *River Res. Appl.*, *25*(4), 367–375.

Poole, G. C., J. A. Stanford, S. W. Running, C. A. Frissell, W. W. Woessner, and B. K. Ellis (2004), A patch hierarchy approach to modeling surface and subsurface hydrology in complex flood-plain environments, *Earth Surf. Processes Landforms*, *29*(10), 1259–1274.

Reeves, G. H., P. A. Bisson, and J. M. Dambacher (1998), Fish communities, in *River Ecology and Management: Lessons from the Pacific Coastal Ecoregion*, edited by R. J. Naiman and R. E. Bilby, Springer, New York.

Runkel, R. L. (1998), One-dimensional transport with inflow and storage (OTIS): a solute transport model for streams and rivers, Water-resources investigations, US Geological Survey, Denver, Colorado.

Saenger, N., P. K. Kitanidis, and R. L. Street (2005), A numerical study of surface-subsurface exchange processes at a riffle-pool pair in the Lahn River, Germany, *Water Resour. Res.*, *41*, W12424, doi:10.1029/2004WR003875.

Salehin, M., A. I. Packman, and M. Paradis (2004), Hyporheic exchange with heterogeneous streambeds: Laboratory experiments and modeling, *Water Resour. Res.*, *40*, W11504, doi:10.1029/2003WR002567.

Savant, A. S., D. D. Reible, and L. J. Thibodeaux (1987), Convective transport within stable river sediments, *Water Resour. Res.*, *23*(9), 1763–1768, doi:10.1029/WR023i009p01763.

Sheibley, R. W., A. P. Jackman, J. H. Duff, and F. J. Triska (2003), Numerical modeling of coupled nitrification–denitrification in sediment perfusion cores from the hyporheic zone of the Shingobee River, MN, *Adv. Water Resour.*, *26*, 977–987, doi:10.1016/S0309-1708,03)00088-5.

Smith, J. W. N. (2005), Groundwater-surface water interaction in the hyporheic zone, pp. 65, UK Environ. Agency, Bristol, U. K.

Stanford, J. A., and J. V. Ward (1998), The hyporheic habitat of river ecosystems, *Nature*, *335*, 64–65.

Storey, R. G., K. W. F. Howard, and D. D. Williams (2003), Factor controlling riffle-scale hyporheic exchange flows and their seasonal changes in gaining stream: A three-dimensional groundwater model, *Water Resour. Res.*, *39*(2), 1034, doi:10.1029/2002WR001367.

Stuart, T. A. (1953), Spawning migration, reproduction and young stages of loch trout (*Salmo trutta* L.), *Rep. 5*, 39 pp., Freshwater and Salmon Fisheries Res., Edinburgh, Scotland.

Thibodeaux, L. J., and J. D. Boyle (1987), Bedform-generated convective transport in bottom sediment, *Nature*, *325*, 341–343.

Tonina, D. (2005), Interaction between river morphology and intra-gravel flow paths within the hyporheic zone, *Ph.D. dissertation thesis*, 129 pp., Univ. of Idaho, Boise, Idaho.

Tonina, D., and J. M. Buffington (2007), Hyporheic exchange in gravel-bed rivers with pool-riffle morphology: Laboratory experiments and three-dimensional modeling, *Water Resour. Res.*, *43*, W01421, doi:10.1029/2005WR004328.

Tonina, D., and J. M. Buffington (2009a), Hyporheic exchange in mountain rivers I: Mechanics and environmental effects, *Geogr. Compass*, *3*(3), 1063–1086.

Tonina, D., and J. M. Buffington (2009b), A three-dimensional model for analyzing the effects of salmon redds on hyporheic exchange and egg pocket habitat, *Can. J. Fish. Aquat. Sci.*, *66*, 2157–2173.

Triska, F. J., V. C. Kennedy, R. J. Avanzino, G. W. Zellweger, and K. E. Bencala (1989), Retention and transport of nutrients in a third-order stream: Channel processes, *Ecology*, *70*, 1894–1905.

Triska, F. J., J. H. Duff, and R. J. Avanzino (1993), The role of water exchange between a stream channel and its hyporheic zone in nitrogen cycling at the terrestrial-aquatic interface, *Hydrobiologia*, *251*, 167–184.

Valett, H. M., J. A. Morrice, C. N. Dahm, and M. E. Campana (1996), Parent lithology, surface-groundwater exchange, and nitrate retention in headwater streams, *Limnol. Oceanogr.*, *41*(2), 333–345.

Vaux, W. G. (1962), Interchange of stream and intragravel water in a salmon spawning riffle, special scientific report, 11 pp., US Fish and Wildlife Serv., Bur. of Commercial Fisheries, Washington, D. C.

Vaux, W. G. (1968), Intragravel flow and interchange of water in a streambed, *Fish. Bull.*, *66*(3), 479–489.

Vittal, N., K. G. Ranga Raju, and R. J. Garde (1977), Resistance of two-dimensional triangular roughness, *J. Hydraul. Res.*, *15*(1), 19–36.

Vronskiy, B. B. (1972), Reproductive biology of the Kamchatka River chinook salmon (*Oncorhynchus tshawytscha* (Walbaum)), *J. Ichthyol.*, *12*, 259–273.

Wagner, B. J., and J. W. Harvey (1997), Experimental design for estimating parameters of rate-limited mass transfer: Analysis of stream tracer studies, *Water Resour. Res.*, *33*(7), 1731–1741, doi:10.1029/97WR01067.

Winter, T. C., J. W. Harvey, O. L. Franke, and W. M. Alley (1998), Ground water and surface water a single resource, circular, U.S. Geological Survey, Denver, Colorado.

Woessner, W. W. (2000), Stream and fluvial plain ground water interactions: Rescaling hydrogeologic thought, *Ground Water*, *38*(3), 423–429.

Wörman, A., A. I. Packman, H. Johansson, and K. Jonsson (2002), Effect of flow-induced exchange in hyporheic zones on longitudinal transport of solutes in streams and rivers, *Water Resour. Res.*, *38*(1), 1089, doi:10.1029/2001WR000769.

Zaramella, M., A. I. Packman, and A. Marion (2003), Application of the transient storage model to analyze advective hyporheic exchange with deep and shallow sediment beds, *Water Resour. Res.*, *39*(7), 1198, doi:10.1029/2002WR001344.

Zarnetske, J. P., M. N. Gooseff, B. W. G. Bowden, J. Morgan, T. R. Brosten, J. H. Bradford, and J. P. McNamara (2008), Influence of morphology and permafrost dynamics on hyporheic exchange in arctic headwater streams under warming climate conditions, *Geophys. Res. Lett.*, *35*, L02501, doi:10.1029/2007GL032049.

J. M. Buffington, Rocky Mountain Research Station, U.S. Forest Service, 322 E. Front St., Ste. 401, Boise, ID 83702, USA.

D. Tonina, Center for Ecohydraulics Research, College of Engineering-Boise, University of Idaho, 322 E. Front St., Ste. 340, Boise, ID 83702, USA. (dtonina@uidaho.edu)